ISSN 1070-4272, Russian Journal of Applied Chemistry, 2009, Vol. 82, No. 11, pp. 1939−1943. © Pleiades Publishing, Ltd., 2009.
Original Russian Text © R.D. Apostolova, O.V. Kolomoets, E.M. Shembel', 2009, published in Zhurnal Prikladnoi Khimii, 2009, Vol. 82, No. 11, pp. 1790−1794.

APPLIED ELECTROCHEMISTRY AND CORROSION PROTECTION OF METALS

Electrolytic Iron Sulfides for Thin-Layer Lithium-Ion Batteries

R. D. Apostolova, O. V. Kolomoets, and E. M. Shembel'

Ukrainian State University of Chemical Engineering, State Higher-Education Institution, Dnepropetrovsk, Russia

Received February 19, 2009

Abstract—Thin-layer electrolytic iron sulfides synthesized on stainless steel substrates were studied in prototype lithium and lithium-ion batteries with an electrolyte composed of ethylene carbonate, dimethyl carbonate, and 1 M $LiClO_4$. A two-volt lithium-ion system with electrolytic iron sulfide and $LiCoO_2$ as negative and positive electrodes, respectively, was suggested. The discharge capacity of the prototype system is 350–400 mA h g^{-1} Fe sulfide.

DOI: 10.1134/S107042720911007X

Studies of Co and Ni sulfides in electrodes of chemical power cells (CPCs) have become rather topical recently and their number is steeply increasing [1–4]. Among subjects of such studies, sulfides of transition metals (M = Co, Ni, Fe, Mo), electrolytically synthesized by the authors in a previous study, are attractive because of the possibility of their use in thin-layer lithium batteries [5].

Electrolytic (e) Fe, Co, and Ni sulfides were tested in cathodes of prototype lithium batteries. e-Fe sulfides deposited onto an aluminum substrate were studied at voltages of 2.8–1.1 with a liquid-phase electrolyte, as well as with gel polymeric electrolytes based on polyvinylidene fluoride and polyvinyl chloride. A discharge capacity of 200–320 mA h g^{-1} in 40–50 cycles, depending on the phase composition of the starting sulfide, has been obtained in thin layers of electrolytic iron sulfides with a mass of 1.0–7.5 mg cm^{-2} in galvanostatic cycling in an electrolyte composed of propylene carbonate (PC), dimethoxyethane (DME), and 1 M $LiClO_4$ [6]. A discharge capacity of 240–300 mA h g^{-1} has been obtained for electrolytic iron sulfides with structures Fe_3S_4 and FeS in prototype lithium batteries with gel-type electrolytes based on polyvinyl chloride, $LiClO_4$, $LiCF_3SO_3$, or $LiN(CF_3SO_2)_2$ salts, and PC plasticizer [7] which is close to the values for a liquid-phase electrolyte. Iron sulfide formulations in prototype lithium CPCs with gel-type polyvinylidene fluoride electrolytes are capable of an electrochemical transformation to yield 200–280 mA h g^{-1} in 80–180 cycles [8].

Electrolytic Co and Ni sulfides have been used, similarly to e-Fe sulfides, in positive electrodes of prototype lithium batteries in the range 2.8–1.1 V [9]. Then, the range of voltages in battery cycling was extended to values possible for negative electrodes of lithium-ion systems. In a prototype lithium power cell with an alkyl carbonate electrolyte, a discharge capacity of 250–450 mA h g^{-1} was obtained for electrolytic cobalt sulfide e-Co9S 8 at voltages of 2.80–0.02 V [10]. In a prototype CPC with an electrolyte composed of ethylene carbonate (EC), dimethyl carbonate (DMC), and 1 M $LiClO_4$, electrolytic nickel sulfide provides a capacity of 400 mA h g^{-1} at 50th cycle in discharge-charge galvanostatic cycling (I_{dis} = 25 mA g^{-1}) at voltages of 2.80–0.01 V relative to lithium at room temperature [11].

In the present study, the range of working voltages in cycling of electrolytic iron sulfides is also extended and their ability to undergo multiple effective electrochemical transformations in negative electrodes of the lithium-ion system is revealed.

EXPERIMENTAL

Iron sulfides conditionally designated e-F_xS_y were

electrolytically synthesized from aqueous solutions of iron(II) sulfate in the presence of thiosulfate ions on a 18N12Kh9T stainless steel substrate. Aluminum substrates were used to obtain electrolytic iron sulfides of the series Fe_3S_4, FeS, FeS_2, Fe_4S_3, etc. [6], which cannot be used in the lithium-ion system at low potentials because of the substrate disintegration via electrochemical intercalation of lithium into aluminum. Therefore, e-Fe sulfides for the lithium-ion system were deposited onto a stainless steel substrate, which is inactive in the electrochemical reaction with lithium. A wide variety of iron sulfide phases was obtained in this case, as it was also done with the aluminum substrate, by varying the electrolysis parameters. In this study, the iron sulfide composite synthesized in an electrolyte containing (g l^{-1}) 13–15 $FeSO_4 \cdot 7H_2O$ and 5.0–5.5 $Na_2S_2O_3 \cdot 5H_2O$ at room temperature, pH 3.8–4.2, and i_{cath} = 2 mA cm^{-2} was examined.

The surface morphology and profile were studied on a Digital Instruments Nanoscop 111-a Dimention atomic-force microscope (AFM). The phase composition of the deposits was found from X-ray diffraction patterns obtained on a DRON-2.0 diffractometer, with a LiF crystal as monochromator (CoKα radiation).

The electrochemical characteristics of e-Fe_xS_y were studied in a prototype disc CPC 2325 with a lithium counter electrode, and also in pair with a $LiCoO_2$ electrode at room temperature. An electrolyte composed of a 1 : 1 (v/v) EC : DMC mixture (Merck, Germany) and 1 M $LiClO_4$ (Iodobrom, Ukraine) was used in the prototypes. The water content of the electrolyte, found by the Fisher method, did not exceed 0.005%. Lithium plates with an excess mass were used in anodes of the prototype lithium CPC. The positive composite $LiCoO_2$ electrode included (%) 80 $LiCoO_2$, 10 acetylene black, and 10 F_4 fluoroplastic binder. It was fabricated by the conventional pasting method by deposition of the active material (7–9 mg cm^{-2}) onto an aluminum current collector. $LiCoO_2$ was synthesized thermally by sintering a stoichiometric mixture of Li_2CO_3 and Co_3O_4. The discharge capacity of such an electrode is 130 mA h g^{-1} at 5th cycle. The prototype cells were assembled in a glove box in dry argon. The galvanostatic cyclic of the prototype cells was performed on a test stand equipped with appropriate software.

The surface structure and morphology of electrolytic iron sulfide deposits depend on technological parameters of the electrolysis and on the substrate nature. The X-ray diffraction pattern of the electrolysis product synthesized under the conditions specified (Fig. 1) indicates that the material under study contains sulfides with Fe_3S_4 and FeS structures and an insignificant admixture of iron oxide β-Fe_2O_3.

Compact deposits of an electrolytic iron sulfide formulation on a stainless steel substrate have the form of dark brown, dark gray, and even black layers. AFM images of the surface of the deposits show that grains in a deposit are grouped into spheroid formations (200–300 nm) (Fig. 2). There are growth steps reproducing the substrate profile on the deposit surface.

In cycling in a prototype lithium CPC at voltages of 2.8–1.1 V for more than 50 cycle, the e-Fe_xS_y electrode with 1.0–1.5 mg cm^{-3} of the active material (Fe_3S_4, FeS, β-Fe_2O_3) has stable discharge-charge characteristics (Fig.3a), with a discharge capacity as high as 500 mA h g^{-1}.

The theoretical specific capacities for the reactions in which e-Fe_xS_y interacts with lithium, (**I**) and (**II**), are 610 and 725 mA h g^{-1}, respectively:

$$FeS + 2Li^+ + 2e \rightarrow Li_2S + Fe, \quad (I)$$

$$Fe_3S_4 + 8Li^+ + 8e \rightarrow 4Li_2S + 3Fe. \quad (II)$$

The electrolytic formulation composed of Fe_3S_4, FeS, and β-Fe_2O_3 also exhibited a capacity for cycling at voltages of 2.8–0.02, as shown in Fig. 3b. The differential capacity curves for the sulfide e-Fe_xS_y (Fig. 4) show that the electrochemical reaction of its interaction with lithium

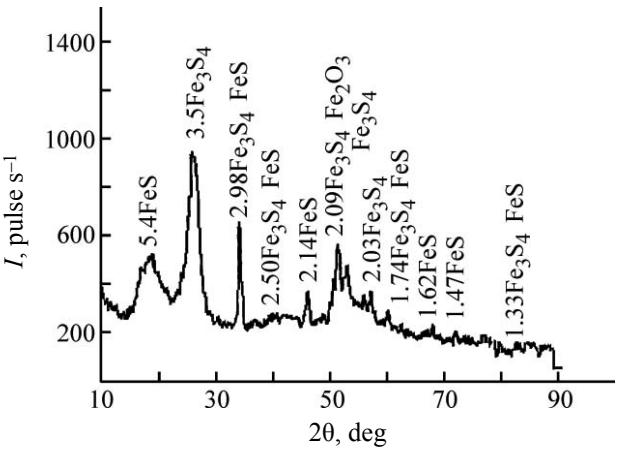

Fig. 1. X-ray diffraction pattern of an e-Fe_xS_y deposit dried in a vacuum at t = 180°C. (2θ) Bragg angle and (I) intensity.

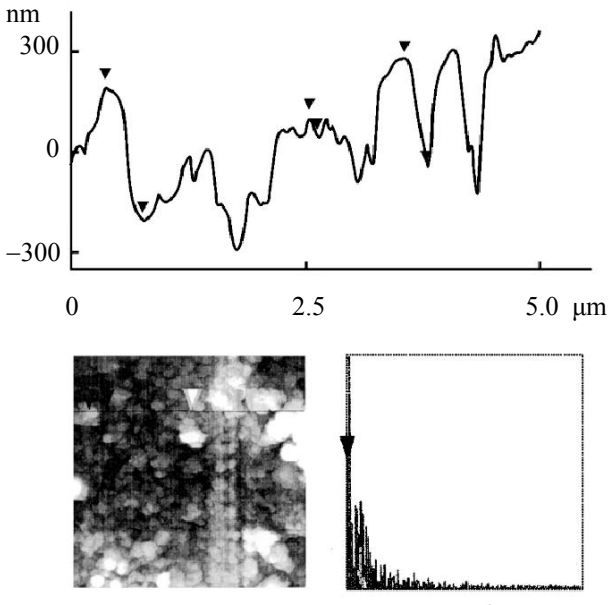

Fig. 2. AFM image of the surface of an e-Fe_xS_y deposit with a mass of 1.8 mg cm^{-2}.

includes several stages occurring at potentials of 2.0, 1.4, and 0.8 V in the cathodic process (lithium intercalation) and 1.0, 1.4, 2.0, and 2.4 in the anodic process (lithium deintercalation). To degrading stages of the discharge-charge process with e-Fe_xS_y belong the stage of lithium intercalation at 0.8 V and stages of lithium deintercalation at 1.0 and 1.4 V. Similar degradation processes have been observed in an electrochemical interaction of an electrolytic sulfide, Co_9S_8, with lithium [10] under the cycling conditions used in the present study. According to published data, the discharge-charge process with MX compounds (X = O, S, F, N) at potentials of 0.8–0 V yields a solid-electrolyte film on particles of the active material as a result of its interaction with the electrolyte. The process of film formation is partly reversible [10, 12, 13].

The discharge-charge characteristics of the system $LiCoO_2$/(EC, DMC, 1M $LiClO_4$)/e-(Fe_3S_4, FeS, β-Fe_2O_3) are shown in Fig. 5. The mass of the positive electrode in this system is excessive, the discharge capacity of the system is limited by the negative electrode. The system is a 2-V battery working at voltages of 3.1–1.4 V. Its discharge capacity, equal to 450 mA h g^{-1} in the first cycle, stabilizes at 350–400 mA h g^{-1} after the 15th cycle.

The dependence of the discharge capacity of the 2-V battery on the discharge rate is shown in Fig. 6.

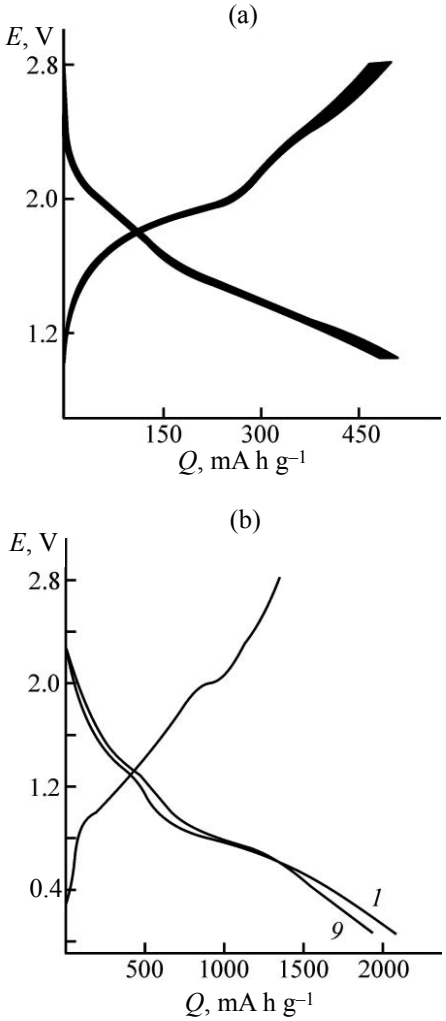

Fig. 3. Discharge-charge characteristics of a prototype e-(Fe_3S_4, FeS, β-Fe_2O_3)/(EC, DMC, 1 M $LiClO_4$)/Li. $i_{dis} = i_{ch} = 0.05$ mA cm^{-2}. (*E*) Voltage of the system and (*Q*) capacity; the same for Fig. 5. (a) 5th–48th cycles, (b) digits at curves are cycle numbers.

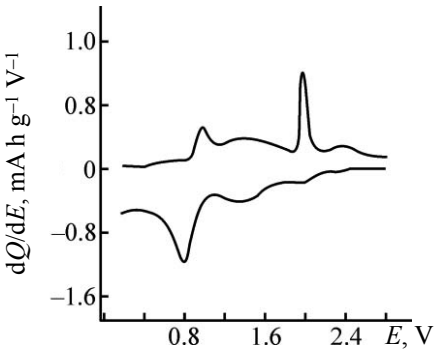

Fig. 4. Differential capacity d*Q*/d*E* vs. the potential E of the sulfide e-Fe_xS_y.

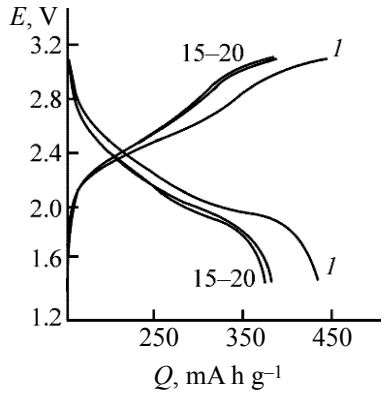

Fig. 5. Discharge-charge curves for the prototype $LiCoO_2$/(EC, DMC, 1 M $LiClO_4$)/e-(Fe_3S_4, FeS, β-Fe_2O_3) for 1st–20th cycles.

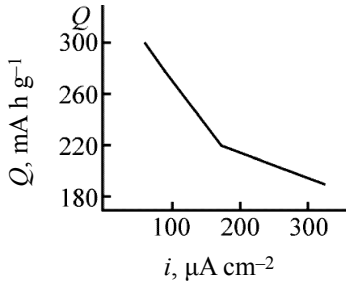

Fig. 6. Discharge capacity Q vs. the discharge rate i for the prototype $LiCoO_2$/(EC, DMC, 1 M $LiClO_4$)/e-(Fe_3S_4, FeS, β-Fe_2O_3) after 30th cycle.

As is known, the attractive distinctive features of iron sulfides among transition metal sulfides are the high specific energy (1270 W h kg^{-1} for FeS_2), comparatively low cost, and low toxicity. The natural and synthetic pyrite FeS_2 shows a high reversibility and an excellent characteristics in lithium batteries at 400–450°C (200Whkg^{-1}) [14]. Attempts have been made to improve the reversibility of pyrite in polymeric medium-temperature (55–140°C) lithium batteries [15]. Its reversibility at room temperature is limited [16, 17]. It can be seen in this context that the results obtained in the present study for electrolytic iron sulfides reversibly working at room temperature in a liquid-phase electrolyte are more successful. The reversible part of the electrochemical transformation of e-Fe_xS_y in prototype lithium CPCs at voltages in the range 2.8–0.02 is 75–80%. It may appear useful to introduce additives into the electrolyte of a power cell to make parasitic reactions less important [18].

CONCLUSIONS

Because the actual discharge capacity of graphite (C) in the conventional commercial lithium-ion system $LiCoO_2$/C is close to 300 mA h g^{-1} (theoretical value 372 mA h g^{-1}), electrolytic iron sulfides providing a discharge capacity of 350–400 mA h g^{-1} in the lithium-ion system can be recommended for further optimization of thin-layer negative electrodes in lithium-ion systems.

ACKNOWLEDGMENTS

The study was financially supported by the Ministry of Education and Science of Ukraine (contract no. 42070390).

REFERENCES

1. Han Sang-Cheol, Kim Hyun-Seok, Song Min-Salg, et al., *J. Alloys Compd*., 2003, vol. 349, pp. 290–296.
2. Wang, J., Ng, Sh., Wang, G.X., et al., *J. Power Sources*, 2006, vol. 159, no. 1, pp. 287–290.
3. Xiujian Zhu, Zhaoyin Wen, Zhonghua Gu, and Shahua Huang, *J. Electrochem. Soc.,* 2006, vol. 153, no. 3, pp. A504–A507.
4. Wang Jia Zhao, Chou Shu-Lei, Chew Sau-Yen, et al*., Solid State Ionics*, 2008, vol. 179, no. 31, pp. 2379–2382.
5. Nagirnyi, V.M., Apostolova, R.D., and Shembel', E.M., *Sintez i elektrokhimicheskie kharakteristiki elektroliticheskikh metallo-oksidnykh i metallo-sul'fidnykh materiallov dlya litievykh akkumulyatornykh sistem* (Synthesis and Electrochemical Characteristics of Electrolytic Metal Oxide and Metal Sulfide Materials for Lithium Battery Systems), Dnepropetrovsk: Ukr. State Univ. Chem. Eng., State High-Educ. Institution, 2008.
6. Shembel', E.M., Apostolova, R.D., Nagirnyi, V.M., et al., *Elektrokhimiya*, 2004, vol. 40, no. 7, pp. 843–851.
7. Apostolova, R.D., Neduzhko, L.I., and Shembel', E.M., *Zh. Prikl. Khim*., 2008, vol. 81, no. 6, pp. 939–944.
8. Apostolova, R.D., Shembel', E.M., and Kolomoets, O.V., *Elektrokhim. Energet*., 2009, vol. 9, no. 4, pp. 237–240.
9. Apostolova, R., Shembel, E., Talyosef, Y., et al*., Advanced Batteries and Accumulators*, ABA-2007, Brno, 2007, pp. 23–26.
10. Apostolova, R., Shembel', E., Talyosef, Y., et al., *Elektrokhimiya*, 2009, vol. 45, no. 3, pp. 330–339.
11. Apostolova R., Maksjuta I., Shembel E. et al., *Russia–Japan Seminar on Advanced Materials and Processing*,

Novosibirsk, 2007, pp. 97–100.

12. Gireaud, G., Grugeon, S., Laruelle, S., et al., *J. Electrochem. Soc*., 2005, vol. 152, no. 5, pp. A850–A857.
13. Novak, P., Wьrsig, A., Buqa, H., et al., *Lithium Batteries Discussions: Electrode Materials*, Arcachon, France, 2005, p. 178.
14. Tomczuk, Z., Tani, B., Otto, N.C., et al*., J. Electrochem. Soc*., 1982, vol. 129, no. 5, pp. 925–931.
15. Strauss, E., Golodnitsky, D., and Peled, E., *Electrochim. Acta*, 2000, vol. 45, pp. 15–19.
16. Apostolova, R.D. and Shembel', E.M., *Zh. Prikl. Khim*., 1995, vol. 68, no. 9, pp. 1483–1487.
17. Bannik, N.G., Neduzhko, L.I., and Shembel', E.M., *Vopr. Khim. Khim*. Tekhnol., 2005, no. 3, pp. 152–155.
18. Aurbach, D., Talyosef, Y., Markovsky, B., et al*., Electrochim. Acta,* 2004, vol. 50, pp. 247–254.